

College of Saint Benedict and Saint John's University

DigitalCommons@CSB/SJU

---

Honors Theses, 1963-2015

Honors Program

---

2014

## Measuring Ultrashort Laser Pulses Using Frequency-Resolved Optical Gating in Conjunction with Genetic and Iterative Algorithms

Alexandra M. Brancale

*College of Saint Benedict/Saint John's University*

Follow this and additional works at: [https://digitalcommons.csbsju.edu/honors\\_theses](https://digitalcommons.csbsju.edu/honors_theses)



Part of the [Physics Commons](#)

---

### Recommended Citation

Brancale, Alexandra M., "Measuring Ultrashort Laser Pulses Using Frequency-Resolved Optical Gating in Conjunction with Genetic and Iterative Algorithms" (2014). *Honors Theses, 1963-2015*. 33.

[https://digitalcommons.csbsju.edu/honors\\_theses/33](https://digitalcommons.csbsju.edu/honors_theses/33)

This Thesis is brought to you for free and open access by DigitalCommons@CSB/SJU. It has been accepted for inclusion in Honors Theses, 1963-2015 by an authorized administrator of DigitalCommons@CSB/SJU. For more information, please contact [digitalcommons@csbsju.edu](mailto:digitalcommons@csbsju.edu).

**Measuring Ultrashort Laser Pulses using Frequency-Resolved Optical Gating in  
Conjunction with Genetic and Iterative Algorithms**

AN HONORS THESIS

College of Saint Benedict/Saint John's University

In Partial Fulfillment

of the Requirements for All College Honors  
and Distinction

in the Department of Physics

by

**Alexandra M. Brancale**

April, 2014

**PROJECT TITLE: Measuring Ultrashort Laser Pulses using Frequency-Resolved Optical Gating in Conjunction with Genetic and Iterative Algorithms**

Approved by:

Adam Whitten  
Adjunct Assistant Professor of Physics

Yu Zhang  
Associate Professor of Computer Science

Dean Langley  
Chair, Department of Physics

Anthony Cunningham  
Director, Honors Thesis Program

## **Abstract**

Precise ultrashort light pulse measurements are critical in many physics experiments using ultrafast lasers. A Frequency-Resolved Optical Gating (FROG) system can efficiently and accurately record these desired measurements. FROGs split the input laser beam, delay half of the beam, and overlap both halves in a nonlinear medium. The resulting beam allows the retrieval of phase and duration information. A data file is created by the FROG software that includes beam intensity measurements. By using genetic and iterative algorithms, the intensity data can be manipulated in order to retrieve the pulse duration and phase information. One focus of this research was to align the FROG and crosscheck the measurements with a commercially-built FROG. The other component of this research was to determine a way to interpret intensity data from the laser using genetic and iterative algorithms together. Correct interpretations of the intensity data result in pulse duration and phase measurements.

## Introduction

In today's physics laboratories around the world, precise duration and phase measurements of ultrashort laser pulses are becoming increasingly important for technical experiments. Ultrashort laser pulses can have a duration on the order of picoseconds,  $10^{-12}$  seconds, or less. However, modern electronic measuring devices are unable to accurately detect events shorter than the picosecond range (Trebino, 2000, p. 4). Technically, in order to measure the duration of any event, an even shorter event is required. But how can one measure the shortest events ever created (Trebino, 2000, p. 1)? The solution is to gate the pulse with itself; thus, a new measurement technique was created.

Before discussing the measurement techniques used today, it is important to look at why these pulse measurements are essential to researchers. Any experiment that uses lasers to manipulate or vibrate specific molecules requires extensive information about the actual laser pulse being used. The more that is known about the pulse exciting the molecules, the more one can understand and describe the molecular dissociation or vibration that occurs (Trebino, 2000, p. 2). Duration, phase, and variation of frequency in an ultrashort pulse can have significant impacts on the outcome of an experiment. Variation in the frequency of an ultrashort laser pulse over time is commonly referred to as a chirp. See Fig. 1 below for a visual representation of a chirped ultrashort laser pulse. A chirped pulse can greatly increase the photo-dissociation of a molecule, which can skew the results of an experiment (Trebino, 2000, p. 2).

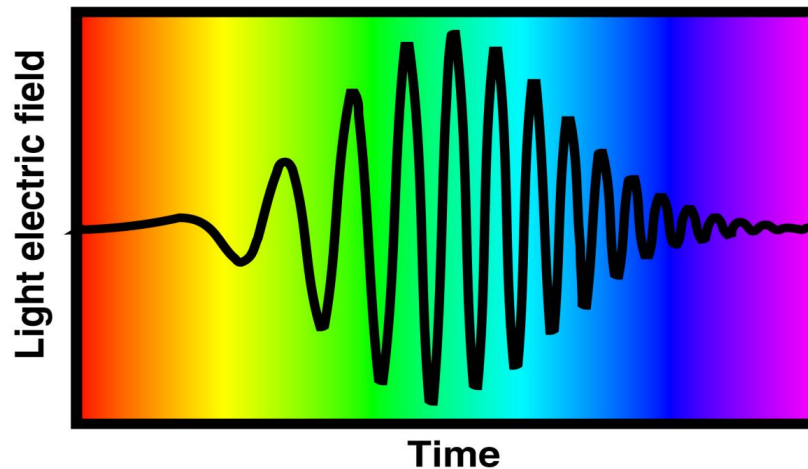


Figure 1. Above is a visual representation of frequency variation in time of a laser pulse. From the red section to the blue section of the spectrum for this pulse, the frequency increases linearly. This frequency variation in time is commonly called a chirp. Image Credit: Trebino, 2014b.

Not only does knowing more about a laser pulse assist with the execution of precise experiments, it also has the potential to tell researchers about the laser itself. Details about an ultrashort laser pulse can help experimenters understand the distortions and limits of the laser with which they are working. Generally, a better understanding of the ultrashort pulses and the mode-locked lasers that create those pulses leads to the generation of even shorter laser pulses (Trebino, 2000, p. 2).

Mode-locked lasers are necessary to create ultrashort laser pulses because they produce consistent, in-phase harmonic frequencies that constructively interfere with each other producing a single, intense ultrashort pulse (Trebino, 2014a). See Fig. 2 below for a visual representation of how mode locking produces ultrashort laser pulses.

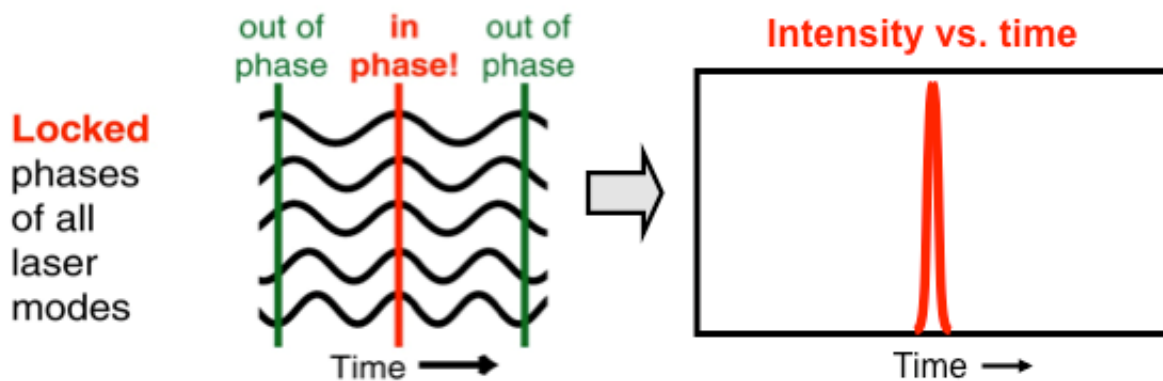


Figure 2. The above figure shows how all of the harmonic frequencies of a mode-locked laser constructively interfere in order to produce an ultrashort laser pulse. The harmonic frequencies produced by a laser are represented with the waves on the left, and the resulting ultrashort pulse is displayed in the intensity versus time plot on the right Image Credit: Trebino, 2014a.

The ultrashort laser pulses discussed in this paper were in the femtosecond or  $10^{-15}$  second range. However, as of 2012, the shortest ultrashort laser pulse recorded was 67 attoseconds or  $67 \times 10^{-18}$  seconds (Sumner, 2012)! All ultrashort laser pulses have extremely large bandwidths. A large bandwidth means that a wide spectrum of wavelengths combined to create the pulse (Trebino, 2000, p. 11). The Fourier transformation is a mathematical tool used to find what frequencies are combined to make an ultrashort laser pulse. By transforming a pulse's electric field in terms of time into a pulse's electric field in terms of frequency, this bandwidth information becomes available. See Fig. 3 below for a visualization of the inverse relationship between the pulse duration and the bandwidth.

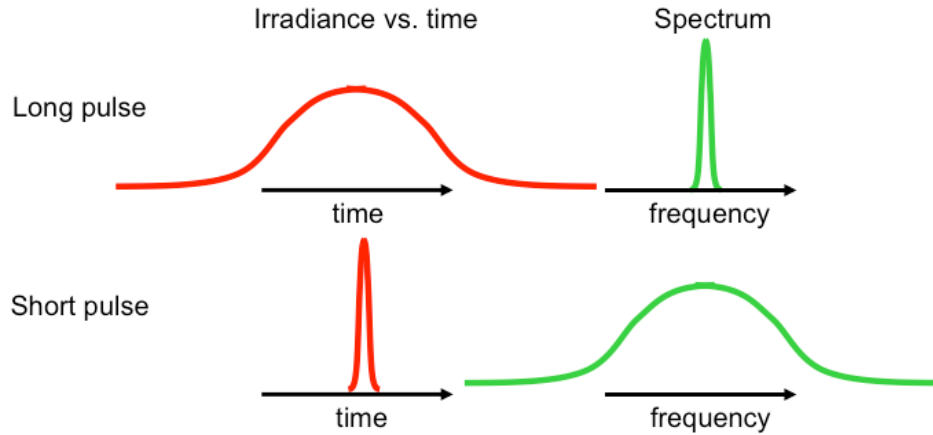


Figure 3. A temporally long pulse has a small bandwidth. That is shown with the top half of the figure. The bottom half of the figure represents an ultrashort pulse and its large bandwidth. The shorter a laser pulse, the larger the bandwidth. Image Credit: Trebino, 2014a.

From the 1960s through the early 1990s, ultrashort laser pulse measurements were made in either the time domain or in the frequency domain. The time domain means that measurements were made with respect to time, and the frequency domain means that measurements were made with respect to the frequency. The time domain measurements were made using a technique called autocorrelation (Wong, 2013, p. 2781). This process involves splitting an ultrashort laser pulse in two, delaying half of the beam, and using the delayed half to measure the stationary half in a nonlinear optical medium (Trebino, 2000, p. 65). Other than the delay in time, the pulses are identical.

When the two initial pulses overlap in the nonlinear medium, a signal pulse is produced. This signal pulse, which is a result of the interaction between the two initial pulses, is then sent into a detector. Intensity information about the signal pulse can be obtained only when the pulses are precisely overlapped in time and space within the nonlinear medium since the detector yields nonzero results only when the overlap occurs

(Trebino, 2014d). Typically, autocorrelation intensity results display very little information about the shape of the pulse and considerably less substructure than the actual intensity of the pulse it is modeled after (Diels, 1996, p. 367; Trebino, 2014d). These pulse shape ambiguities are partially due to the fact that the intensity autocorrelation is always symmetric with respect to the delay between the pulses, and they make autocorrelation an unreliable method of pulse measurement (Trebino, 2014d).

Through spectrum analysis of the resulting signal pulse, one can obtain basic information about the frequencies making up the pulse. However, spectrum analysis alone yields no information about the variation of frequency throughout the duration of the pulse. This lack of information is a result of spectrum analysis pertaining only to the frequency domain.

Autocorrelation and spectrum analysis measurements come from either the time domain or the frequency domain respectively. Separately, these measurement techniques do not yield the desired, precise information about the laser pulse duration and phase evolution. Thus a hybrid time-frequency domain was considered to remedy these faults. The time-frequency domain had not been commonly used in optics until researchers discovered the need to more precisely measure ultrashort laser pulses (Trebino, 2000, p. 101). In 1991, ultrafast optics was changed by the discovery that spectrally resolving an autocorrelation signal pulse yields both phase and duration information for the initial ultrashort laser pulse (Trebino, 2000, p. 4).

## **Frequency-Resolved Optical Gating (FROG)**

### ***Theory***

Frequency-Resolved Optical Gating (FROG) can successfully and efficiently record pulse characteristics by overlapping a split and partially delayed duplicate laser pulse in a nonlinear optical medium such as a second-harmonic generation (SHG) crystal (Trebino, 2014e). When the pulses are overlapped in the crystal, a frequency-doubled pulse of light is produced that is encoded with the necessary characteristics of the initial laser pulse (Trebino, 2014c).

Nonlinear materials allow beams of light to pass through and affect each other. They also have the ability to convert an intense beam of light into light with a different frequency (Trebino, 2000, p. 37). In the case of an SHG FROG, the nonlinear medium is an SHG crystal. The SHG crystal converts two red, 800 nm photons into one blue, 400 nm photon. The SHG photons have twice the energy and twice the frequency of the initial photons (Trebino, 2014c). The production of SHG light depends on how fully the initial pulses overlap within the crystal.

In an SHG FROG apparatus, the delayed pulse gradually overlaps the stationary pulse throughout the delay, and the resulting SHG signal pulse then spectrally resolved. The signal pulse is diffracted by the spectrometer's grating and recorded on the charged-couple device (CCD) camera. See Fig. 4 below for a schematic diagram showing the path of an ultrafast laser beam through the Kansas State University FROG apparatus.

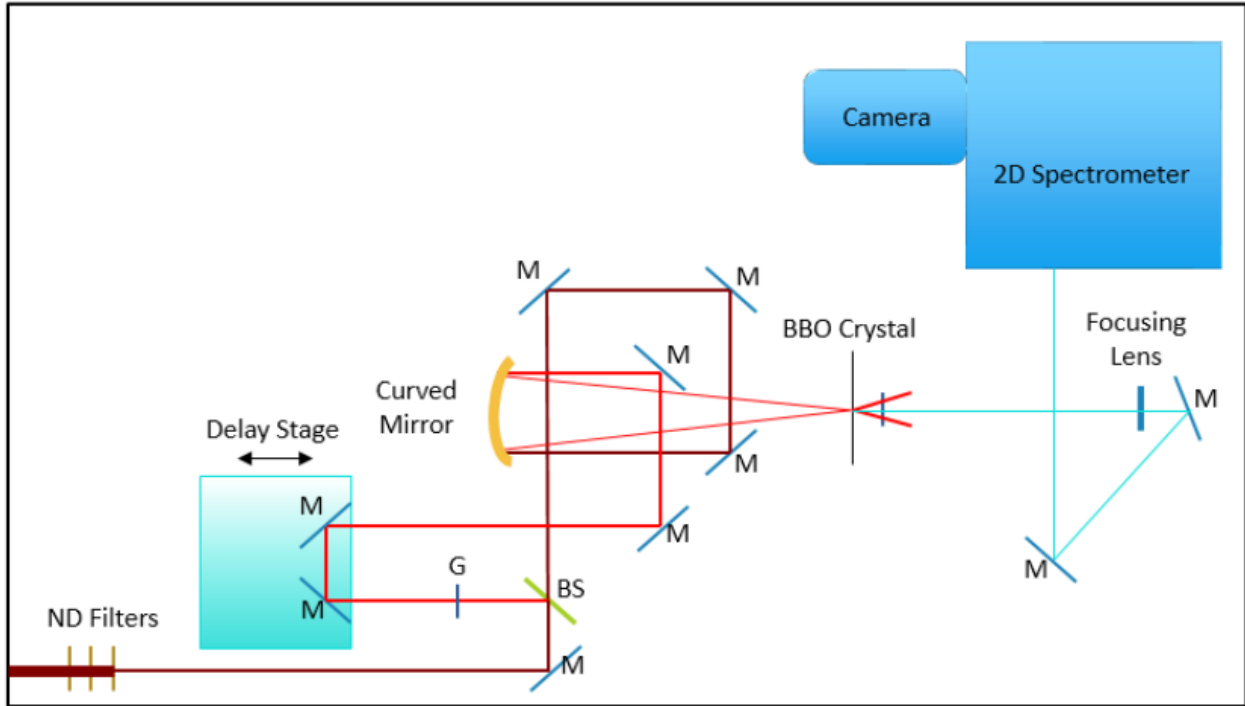


Figure 4. Above is a schematic drawing of the Kansas State University SHG FROG showing the path of the ultrafast laser beam through the apparatus. G stands for glass, M for mirror, BS for beam splitter, and ND for neutral density. The nonlinear SHG crystal in the Kansas State FROG is a BBO crystal. BBO stands for Barium Borate. The arrows above the delay stage indicate the directions in which the stage moves during data collection.

The intensity data from the SHG signal pulse is recorded by the two-dimensional spectrometer and is commonly referred to as a FROG trace. Two-dimensional spectrometers are critical to the retrieval of the intensity and phase information throughout the evolution of the initial pulses' overlap. The signal pulse is spectrally resolved as a function of the time delay  $\tau$  between the split pulses in order to create the FROG trace (DeLong, 1994, p. 2206). A FROG trace is a positive, experimentally recorded, real-valued intensity function dependent on the frequency and time delay between the two pulses (DeLong, 1994, p. 2207). Fig. 5 below is an experimentally collected FROG trace image.

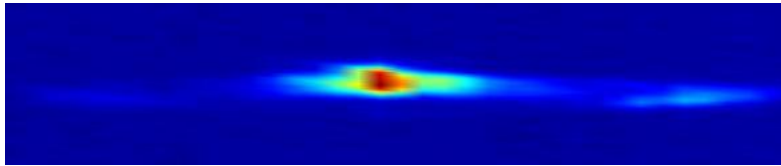


Figure 5. The above image was created by plotting a FROG trace data set with Matlab. The above image is a frequency versus time plot. The color arbitrarily shows intensity of the recorded ultrashort signal pulse.

By analyzing the signal pulse's intensity data, phase and duration information about the initial pulse becomes available. However, there is a flaw with SHG FROG systems that influences the interpretation of traces. The electric field amplitude of the signal pulse in time  $E_{sig}(t, \tau)$  for an SHG FROG is invariant except for a trivial time dependent offset with respect to change in the sign of the delay time  $\tau$ . This unfortunate ambiguity only occurs with SHG FROGs, as is demonstrated in Fig. 6 below and can lead to unintuitive traces. Since SHG FROGs are symmetric about  $\tau$ , this issue will always occur (DeLong, 1994, p. 2207). However, there are methods used to get around the initial ambiguity.

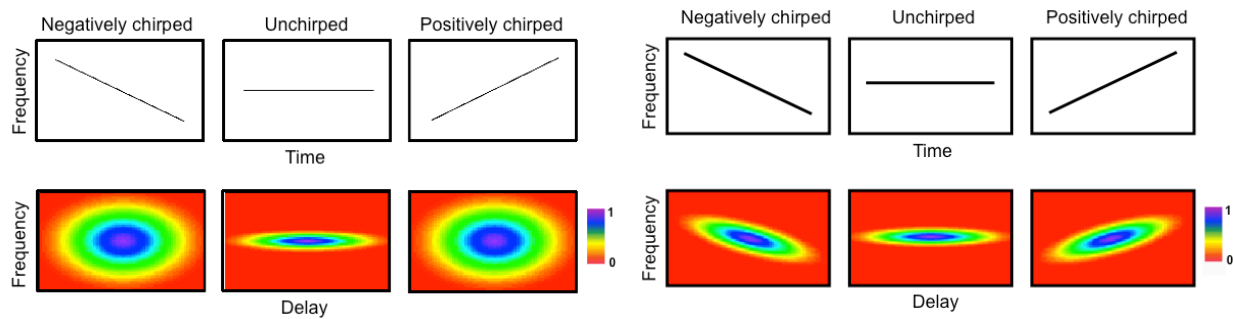


Figure 6. The above figure shows the main ambiguity and downfall in SHG FROG traces. The top, white plots show three different types of frequency variation in time for ultrashort laser pulses. The bottom, colorful plots show what FROG traces typically appear like with the corresponding frequency variation. By comparing the chirped SHG FROG trace examples on the left with the chirped trace examples from a different type of FROG (3<sup>rd</sup> order FROG) on the right, it is apparent that there is temporal vagueness with linearly chirped pulses in SHG FROGs. Image Credit: Trebino, 2014e.

It is important to note that SHG FROGs have this temporal ambiguity only when phase distortions are even functions of time. For example, linear chirps have indistinguishable signs due to the fact that they have a quadratic temporal phase dependence. In contrast, frequency shifts and temporal phase distortions are clearer because they have linear and cubic phases in time respectively. However, all phase distortions that are determined in the frequency domain have ambiguous signs. It is commonly accepted that laser pulses are positively linearly chirped due to propagation through air and the use of normal optical equipment (DeLong, 1994, p. 2208). A method used to diminish this ambiguity is to put a thin piece of glass in the laser beam's path before the beam splitter in the FROG apparatus. By inserting this piece of thin glass, one creates surface reflections that introduce a small, trailing satellite pulse appearing on only one side of the retrieved pulse (Trebino, 1997, p. 3287).

## ***Procedure***

The SHG FROG apparatus used for the research presented in this paper is located in the James R. Macdonald (JRM) Atomic, Molecular, and Optical (AMO) Physics Laboratory at Kansas State University. The goal specified by the Research Experience for the Undergraduate (REU) mentors was to align the FROG pictured below in Fig. 7, record pulse traces using multiple ultrafast lasers in the JRM Laboratory, crosscheck the traces created by the FROG in Fig. 7 with those of a commercially built FROG, and optimize the student-written LabView program controlling the FROG. The SHG FROG in Fig. 7 belongs to Professor Carlos Trallero's research group. His lab room in the JRM Laboratory is called the High Intensity Tunable Source (HITS) room after this group's laser. Therefore, the student-built SHG FROG will be specifically referred to as the HITS FROG.



Figure 7. Above is an actual image of the Kansas State University HITS FROG. Fig. 4 is simply a schematic of this setup.

Research was conducted with the HITS FROG as seen in Fig. 7. The HITS FROG was initially set up but not aligned. Stefan Zigo, a current physics graduate student at Kansas State University and REU mentor, assisted with the task of aligning the HITS FROG. The alignment process consisted of not only directing the beam onto the subsequent mirrors and through lenses of the apparatus, but also of making sure that the two halves of the split beam overlapped within the Barium Borate (BBO) SHG crystal in time and space. All of the lasers used with the HITS FROG in the JRM Laboratory operated at approximately 800 nm.

According to DeLong and Trebino, FROGs do not require extreme aligning due to the fact that they are not interferometric and are usually automatically phase matched (1994, p. 2206). However, the alignment process for the HITS FROG was not trivial and required extreme attention to detail since precise alignment was required before any ultrashort pulse traces could be recorded. By carefully adjusting the tilt of the mirrors and the orientation of the SHG crystal, SHG light was produced as seen below in Fig. 8.



Figure 8. Both of the split 800 nm beams that entered the BBO crystal were overlapped in time and space and can be seen as the two outside red dots on the paper. The 400 nm SHG beam was successfully produced from the overlap and is the middle blue dot.

The 800 nm light from the Titanium Sapphire ultrafast laser that was initially sent into the HITS FROG apparatus produced 400 nm light after being overlapped in the SHG crystal. Aligning any FROG apparatus is more complicated than just making two ultrashort laser pulses travel through a SHG crystal. In order for SHG light to be produced, the two split beams must overlap in the frequency-doubling BBO crystal in time, as is shown below schematically in Fig. 9, and in space. If those conditions are not met, the resulting SHG light will be very faint or will not appear at all. Once the HITS FROG was aligned, SHG light was produced, and small adjustments were made to the various mirror and SHG crystal knobs until the most intense SHG signal light was produced. The brightest, most intense light was qualitatively determined. A bright SHG beam allows researchers to be confident that the

best overlap of the split pulses is occurring. A precise overlap of the split 800 nm pulses will eventually result in the most accurate pulse duration and phase measurements.

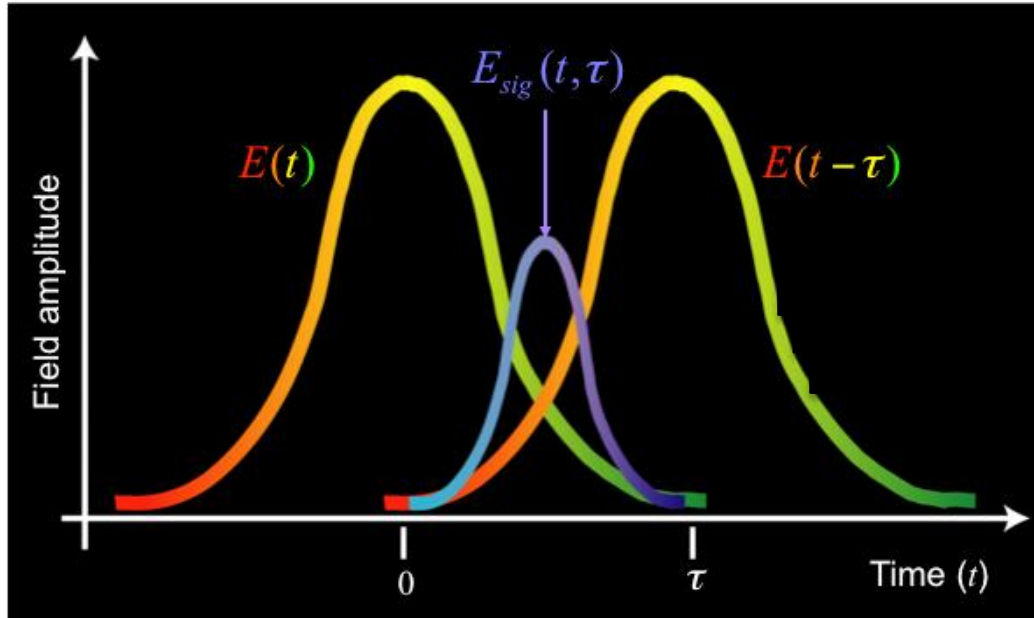


Figure 9. Above is a representation of the amplitude electric fields of the pulse halves overlapping within the SHG crystal. The pulse on the left is the half of the 800 nm pulse that went through the FROG apparatus without being delayed in the delay stage. That half's electric field amplitude is  $E(t)$ . The other half of the 800 nm pulse that was delayed by a time  $\tau$ , has an electric field amplitude  $E(t - \tau)$ . The shorter pulse in the middle is the resulting frequency-doubled 400 nm SHG signal pulse with an electric field amplitude  $E_{sig}(t, \tau)$  dependent both on time  $t$  and delay time  $\tau$ . Image Credit: Trebino, 2014e.

A transform-limited pulse (TLP) is the shortest pulse in time with zero frequency dependence on the spectral phase. TLPs are most commonly used in physics experiments using ultrafast lasers due to the fact that the phase of ultrashort laser pulses can change the outcome of an experiment. These pulses also show the potential of a given laser in terms of the shortest possible pulse duration in time. For FROG apparatus alignment, it is not essential to have a TLP; however, it is beneficial because it allows researchers to visually compare experimentally recorded traces to the expected, symmetrical trace.

In the early stages of the research, full control of the laser was obtained, and adjustments of the laser gratings were allowed in order to use a TLP when collecting FROG traces. Laser gratings allow one to account for the distance the laser beam travels to the experiment. Air is a medium that positively chirps a laser pulse, and by adjusting the grating one can negatively “un-chirp” a laser pulse at a given distance. By changing the gratings of the laser, one can control the distance at which the TLP arrives with zero phase variation. If the HITS FROG was initially calibrated and reliable, the pulse could have been sent into the apparatus to check if the phase throughout the laser pulse at that distance was zero as would be expected for a TLP.

If a FROG apparatus is not calibrated at a given time, the way in which one checks for a TLP requires more steps and avoids using the FROG setup entirely. First, one must set up a focusing lens at a distance away from the laser output that allows the beam to travel the same distance to the FROG’s SHG crystal. One must be careful of the focused beam due to the high amounts of energy focused to one spot. At the focal point of the focusing lens, when the laser gratings are set up correctly, the laser has so much power focused on one small point that plasma will appear since air will be ionized as seen in Fig. 10. Walkie-talkies were used to communicate between the person controlling the laser’s grating and the person watching the focal point since the laser was in a different room than the experimental setup.

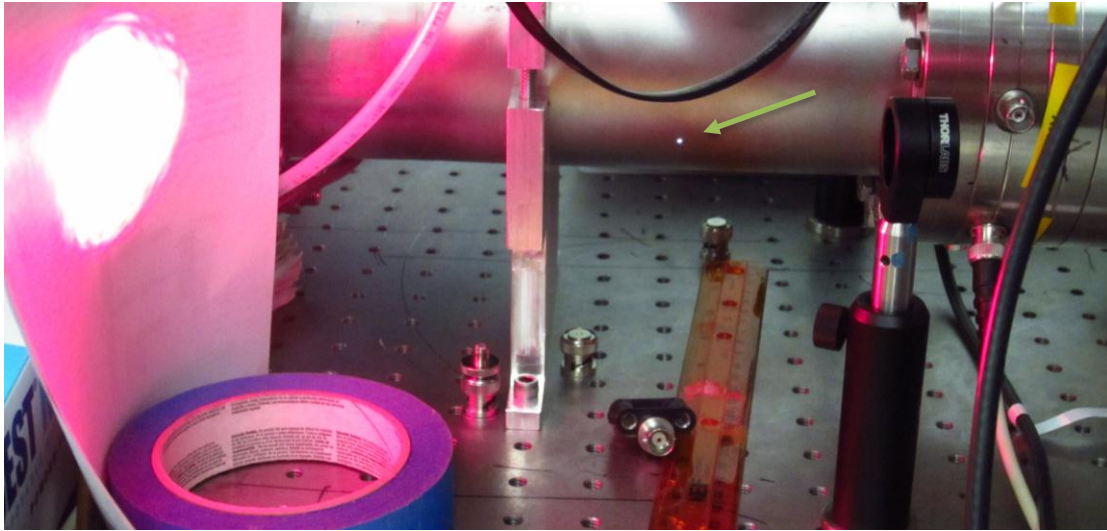


Figure 10. A TLP can ionize air when the laser grating is at the optimal position. The full powered ultrafast laser beam was sent through the focusing Thor labs lens on the right. The green arrow points to the plasma, which is the little white dot in between the lens and the paper.

However, later in the research when the beam had to be shared with other people running experiments, the laser gratings were not allowed to be changed and TLPs were not guaranteed while performing additional alignment and recording traces. Each time a new laser was used with the HITS FROG, the apparatus had to be realigned. This is due to variation in the laser and beam produced. Despite the lack of control, many traces were recorded using the Prairie Ultrafast Laser (PULSAR), another ultrafast laser in the JRM Laboratory.

The program controlling the HITS FROG was written by students in LabView code. The user of this program interacts only with what is called the front panel. This panel consists of buttons, inputs, and tabs that determine how the FROG operates and records a trace. Images, spectrums, and traces recorded by the FROG are displayed on the front panel as well. The code is located on the back panel of the LabView program. The HITS FROG

LabView code is made up of drivers, wires, timers, and many other functions that control the operations of the delay stage, spectrometer, and camera. Modifications were made to the front panel, making the HITS FROG program more user friendly, the controls more obvious, and the settings easier to change. These additional features can be seen below in Fig. 11, which is an example of the front panel of the HITS FROG program.

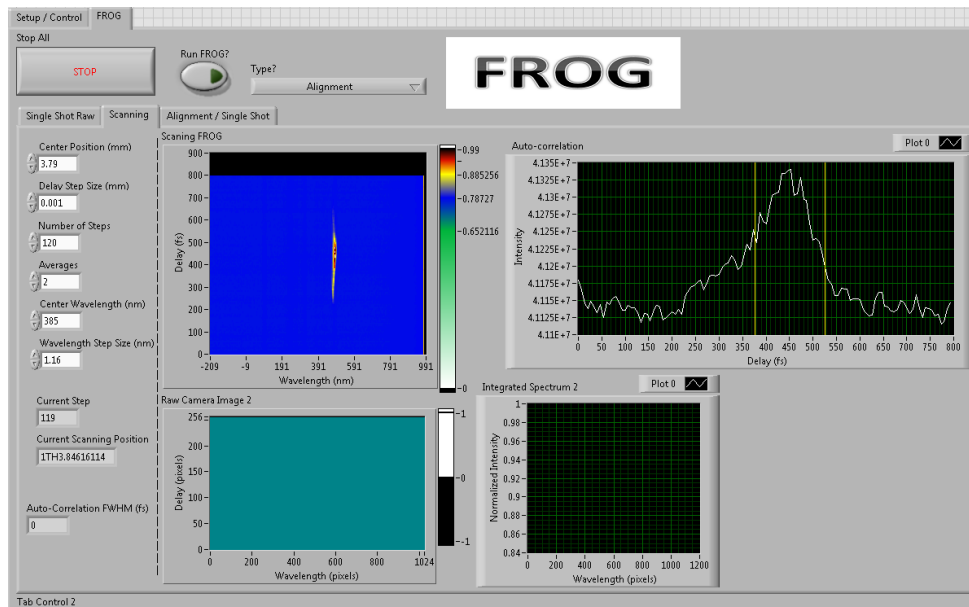


Figure 11. Above is a screenshot of the student-written LabView program that controls the HITS FROG. This screenshot was taken after recording a FROG trace.

A smearing issue was noticed on the raw camera image displayed on the front panel of the HITS FROG LabView program when the FROG was recording signal pulse data in single-shot mode. This issue can be seen in Fig. 12 below.

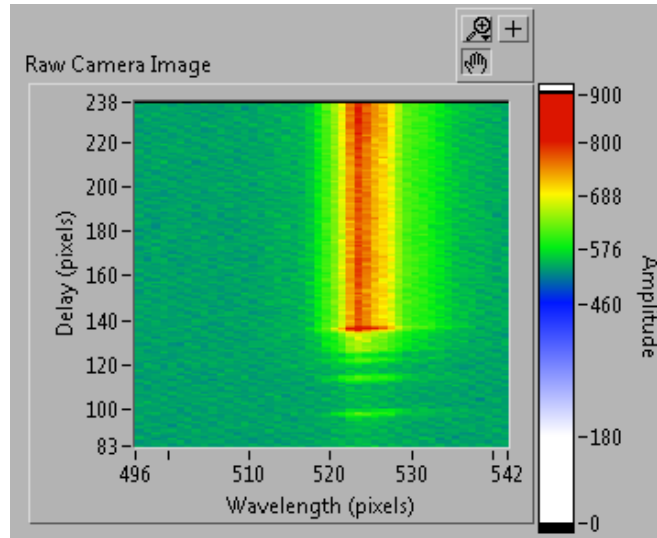


Figure 12. Above is a screenshot of the front panel of the student-written LabView program made to control the HITS FROG. There is a smearing effect occurring on the raw image display that makes it appear as though the pulse is long enough to be stretching off the CCD camera in the vertical direction.

The smearing effect that is apparent in Fig. 12 was thought to have to do with the shutter controls of the CCD camera in the HITS FROG setup. After modifying the code that controls how the CCD camera records images, it was realized that the smearing was a result of poorly timed triggers. The data on the CCD camera's array was not clearing before being read by the program. Therefore, as the data cleared up and off the array, the computer read the results, and the image displayed this smearing effect. During attempts to optimize this LabView program, changes had been made to the timing operations defined in the back panel of the program. In that process, the program began to read the CCD camera too quickly.

Other changes were made to the program that controls the HITS FROG that assisted in reading pulse information and aligning the FROG. A single-shot autocorrelation feature and an alignment mode that displayed live images of the pulse as it was sent into the

spectrometer were added to the HITS FROG program. The autocorrelation feature allowed the user receive an estimate of the pulse duration in a single-shot mode without taking a trace and running the pulse reconstruction software as seen below in Fig. 13. A single-shot mode takes single intensity images from the CCD camera of the intensity of the SHG pulse and displays the plot in real time on the screen. In order to make the best pulse duration estimates, the single-shot mode was utilized during pulse overlaps producing the strongest SHG signal pulse.

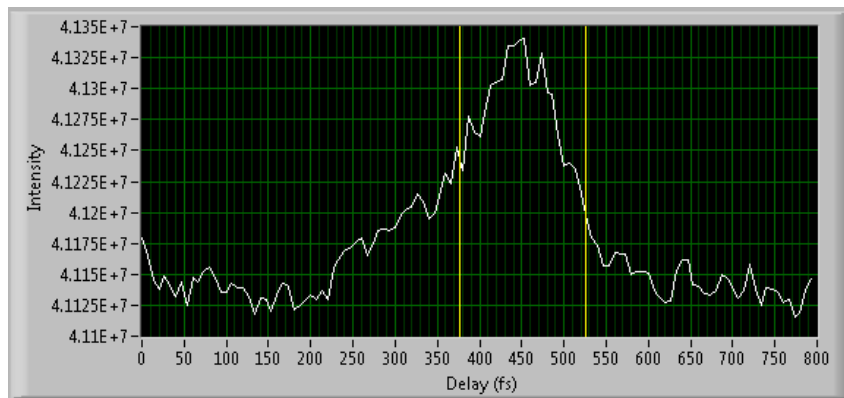


Figure 13. Above is a screenshot taken from the HITS FROG LabView program of the added autocorrelation feature. The difference between the right and the left yellow lines gives a rough estimate as to what the full width at half maximum (FWHM) pulse duration is. This measurement is used as the estimate of the temporal pulse length.

Traces from the HITS FROG and traces from the commercial KM Labs FROG kept in the PULSAR lab room in the JRM Laboratory were compared. The same laser beam was sent through the two FROGs to compare the retrieved pulse measurements for both.

## Pulse Reconstruction

### *Iterative Reconstruction Algorithm*

After a trace is recorded, an iterative pulse reconstruction program employing a numerical algorithm interprets the experimentally collected trace data. The experimental ultrashort pulse is reconstructed so that the reconstruction is as close as possible to the measured pulse. This is achieved by manipulating and interpreting the recorded intensity data. If working correctly, the algorithm eventually determines the full complex electric field of the experimental pulse, which includes the intensity and the phase information of that pulse (DeLong, 1994, p. 2207). By using the experimentally recorded data to direct the reconstruction, the reconstructed pulse can then be modeled by known equations for the electric field and intensity. These equations make the phase and pulse duration measurements obtainable. Phase retrieval is a form of de-convolution because it yields information about the initial pulse that is not originally apparent (Trebino, 2000, p. 109).

There are multiple commercial FROG algorithms, and the goal of each of the programs is to reconstruct the complex electric field amplitude of the initial, split pulse  $E(t)$  using the intensity data in frequency and time of the SHG pulse measured by the experimental FROG trace  $I_{FROG}(\omega, \tau)$  (Trebino, 2000, p. 157). Each FROG trace produces a two dimensional image or spectrogram, on the spectrometer. By recording a series of spectral slices throughout the overlap of the initial pulses, the spectrogram is created (Sullivan, 1996, p. 1966). That spectrogram is mathematically defined as:

$$\Sigma_g^E(\omega, \tau) = \left| \int_{-\infty}^{\infty} E(t)g(t - \tau) \exp(-i\omega t) dt \right|^2$$

Equation 1. (Trebino, 2000, p. 157)

Note that Eqn. 1 is not a summation. That is the typical spectrogram notation used by Trebino and other FROG researchers. Since the FROG setup involves a delayed pulse gating an identical stationary pulse, the gate function  $g(t - \tau)$  in Eqn. 1 is defined as the electric field amplitude of the delayed pulse  $E(t - \tau)$  which is a function of the electric field amplitude  $E(t)$ . Therefore, the intensity of the FROG trace can be more intuitively defined as:

$$I_{\text{FROG}}(\omega, \tau) = \left| \int_{-\infty}^{\infty} E_{\text{sig}}(t, \tau) \exp(-i\omega t) dt \right|^2$$

Equation 2. (Trebino, 2000, p. 157)

The research discussed in this paper only used SHG FROGs, and the specific SHG signal pulse's electric field amplitude is defined by the following proportionality:

$$E_{\text{sig}}(t, \tau) \propto E(t)E(t - \tau)$$

Equation 3. (Trebino, 2000, p. 157)

Eqn. 3 is the result of the overlap of the stationary pulse's electric field amplitude and the delayed pulse's electric field amplitude. Eqn. 2 and Eqn. 3 are critical to the reconstruction algorithm. In Trebino's book, *Frequency-Resolved Optical Gating: The Measurement of Ultrashort Laser Pulses*, the common iterative-Fourier-transform algorithm used to retrieve the phase is presented as is shown below in Fig. 14.

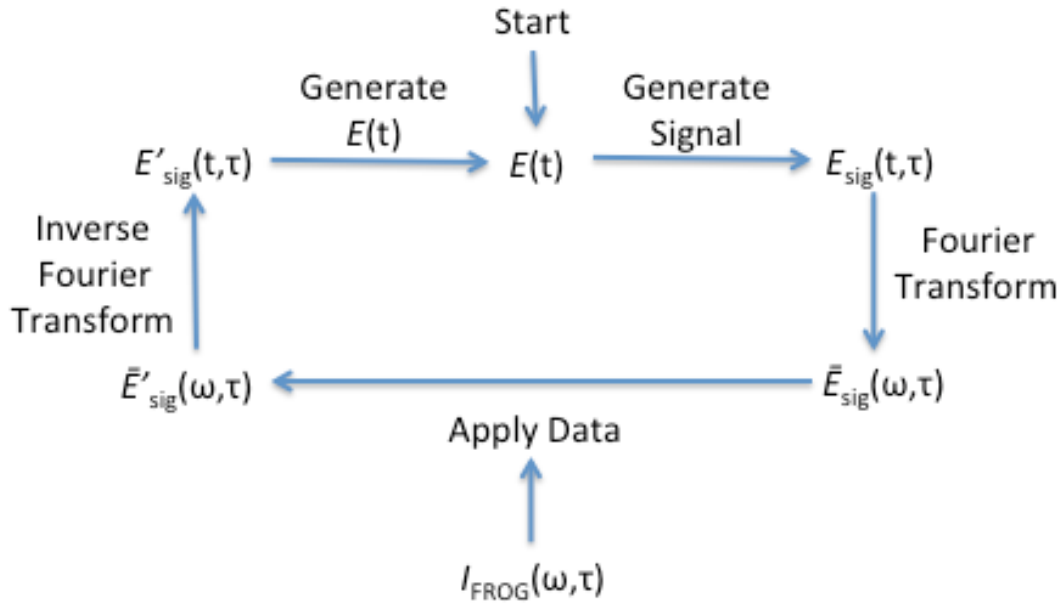


Figure 14. Above is a diagram schematically showing the flow of a typical FROG reconstruction algorithm. The bars signify that a Fourier transformation occurred and the apostrophes signify an improved value. Each time around the loop represents 1 iteration. Adapted From: Trebino, 2000, p. 158.

The algorithm displayed in Fig. 14 begins with a simple initial estimate for the electric field amplitude in time  $E(t)$  of the initial laser pulse (Trebino, 2000, p. 158). This initial electric field amplitude can be estimated in many ways. It can simply be an amplitude electric field of random noise, a Gaussian intensity profile with random phase noise, a Gaussian pulse with zero phase, or even a slightly linearly chirped Gaussian pulse with small satellite pulses trailing behind (DeLong, 1994, p. 2008; Trebino, 2000, p. 160).

After the initial estimate is made, an electric field amplitude of the signal pulse in time  $E_{sig}(t, \tau)$  is generated using Eqn. 3. Next,  $E_{sig}(t, \tau)$  is Fourier transformed with respect to time  $t$  into the frequency domain which yields the signal pulse's electric field amplitude in terms of frequency  $\tilde{E}_{sig}(\omega, \tau)$ . The tilde signifies that the data has undergone a Fourier transformation.

The next step is where the actual experimental FROG trace data is applied. One must realize that the squared magnitude of  $\tilde{E}_{\text{sig}}(\omega, \tau)$  should equal the intensity data collected from the trace  $I_{\text{FROG}}(\omega, \tau)$ . This relationship allows  $\tilde{E}_{\text{sig}}(\omega, \tau)$  to be replaced with the square root of  $I_{\text{FROG}}(\omega, \tau)$ . This substitution occurs at each pixel of the reconstruction and creates an improved signal pulse electric field amplitude in terms of frequency  $\tilde{E}'_{\text{sig}}(\omega, \tau)$ . The apostrophe signifies that the data has been improved (Trebino, 2000, p. 158).

Then,  $\tilde{E}'_{\text{sig}}(\omega, \tau)$  undergoes an inverse Fourier transformation with respect to frequency  $\omega$  back into the time domain yielding an improved electric field amplitude for the signal pulse in time  $E'_{\text{sig}}(t, \tau)$ .  $E'_{\text{sig}}(t, \tau)$  is then used to create a new  $E(t)$  estimate, and the cycle is repeated (Trebino, 2000, p. 158). This loop continues until a tolerance for the error calculation is reached, and that will occur only when  $\tilde{E}_{\text{sig}}(\omega, \tau)$  is considered close enough to  $I_{\text{FROG}}(\omega, \tau)$ .

Trebino developed a basic algorithm used in the initial stages of FROG reconstruction. The basic FROG algorithm uses Eqn. 2 as a data constraint and Eqn. 3 as a mathematical constraint. Satisfying the data constraint in the basic algorithm means updating the estimated electric field amplitude of the signal  $\tilde{E}'_{\text{sig}}(\omega, \tau)$  with the following equation:

$$\tilde{E}'_{\text{sig}}(\omega, \tau) = \frac{\tilde{E}_{\text{sig}}(\omega, \tau)}{|\tilde{E}_{\text{sig}}(\omega, \tau)|} \sqrt{I_{\text{FROG}}(\omega, \tau)}$$

Equation 4. (Trebino, 2000, p. 159)

This equation is used at every iteration of the FROG algorithm when the FROG trace data is applied to the signal pulse's electric field in frequency. If the square root of

$I_{\text{FROG}}(\omega, \tau)$  divided by the absolute value of  $\tilde{E}_{\text{sig}}(\omega, \tau)$  equals or is very close to one, then the current estimate of  $\tilde{E}_{\text{sig}}(\omega, \tau)$  will also act as the improved version of that measurement  $\tilde{E}'_{\text{sig}}(\omega, \tau)$ . At this point in the algorithm, there is no way to improve  $\tilde{E}_{\text{sig}}(\omega, \tau)$ , and the retrieval process is complete. Fulfilling the math constraint is more complicated than the data constraint and is done with the following Eqn. 5. The new electric field in time is determined by an integral:

$$E^{(k+1)}(t) = \int_{-\infty}^{\infty} E_{\text{sig}}^{(k)}(t, \tau) d\tau$$

Equation 5. (Trebino, 2000, p. 159)

In Eqn. 5, the variable  $k$  represents the current iteration number. Then, the error at each iteration of the FROG reconstruction algorithm is determined with the following equation:

$$G^{(k)} = \sqrt{\frac{1}{N^2} \sum_{i,j=1}^N \left| I_{\text{FROG}}(\omega_i, \tau_j) - \mu I_{\text{sig}}^{(k)}(\omega_i, \tau_j) \right|^2}$$

Equation 6. (Trebino, 2000, p. 160)

For Eqn. 6, the variable  $\mu$  is a real normalization constant that minimizes the error,  $I_{\text{FROG}}(\omega_i, \tau_j)$  is the measured FROG trace,  $I_{\text{sig}}^{(k)}(\omega_i, \tau_j)$  is the  $k$ -th iteration of the retrieved FROG trace (also known as the squared magnitude of the  $\tilde{E}_{\text{sig}}^{(k)}(\omega, \tau)$ ),  $\omega_i$  is the  $i$ -th frequency vector, and  $\tau_j$  is the  $j$ -th delay vector (Trebino, 2000, p. 160).  $N^2$  is the total number of pixels on the CCD camera. The value that Eqn. 6 yields is called the FROG error. More specifically, it is the root-mean-square difference between the experimentally measured trace  $I_{\text{FROG}}(\omega_i, \tau_j)$  and the computed trace  $I_{\text{sig}}^{(k)}(\omega_i, \tau_j)$  that results from the last

iteration's electric field in time (Wong, 2013, p. 2784; Trebino, 1997, p. 3291). For variable clarification, refer to the Appendix.

There are disadvantages to using only the basic algorithm to reconstruct pulses. When there is a lot of noise in the experimental trace or the substructure of the intensity pulse is complex, the algorithm is less likely to converge. Despite these faults, this algorithm is still used in the commercial FROG reconstruction program as the initial algorithm because of its ability to quickly zero in on the actual pulse. However, once this algorithm stagnates, other more precise and slower algorithms are called in order to fine-tune the reconstruction (Trebino, 2000, p. 160).

### ***Genetic Algorithm***

It was hypothesized that a genetic algorithm could increase the accuracy and efficiency of the pulse reconstruction process. Genetic algorithms are a type of evolutionary algorithm used in optimization problems with multiple parameters. The algorithm finds the optimal solution to a problem by continuously changing the values of those parameters, evaluating the equation with those parameters, comparing it to the optimal result, and producing a new set of more optimal parameters to be compared to the result.

In terms of genetic algorithms, the particular parameters that are modified are called genes, and the group of genes that acts as a set of parameters is called an individual. In this application of a genetic algorithm to the pulse reconstruction process, an individual would be the initial estimated electric field in time  $E(t)$  of the input ultrashort laser pulse. The different genes of an individual would be numbers that decide the phase, duration, noise, and other commonly measured values of that estimated pulse.

A generation is a group of individuals with a variety of genes, and in this application to pulse reconstruction a generation would be made up of many different initial electric field estimates. Each individual of a generation is then evaluated by the fitness function. The fitness value created by each individual influences the likelihood that the individual will be able to pass on their genes to the next generation as a parent. Genetic algorithms use the evolutionary idea that only the fittest individuals will pass genes to the next generation.

The fitness function for this particular problem could be defined as Eqn. 6. Every individual would begin as  $E(t)$ , change into  $E_{\text{sig}}(t, \tau)$ , and become  $\tilde{E}_{\text{sig}}(\omega, \tau)$  by the methods described in the aforementioned iterative reconstruction algorithm. Finally, that  $\tilde{E}_{\text{sig}}(\omega, \tau)$  would be compared to the square root of the experimentally recorded  $I_{\text{FROG}}(\omega, \tau)$  data. The most fit individuals would have the least discrepancy between their  $I_{\text{FROG}}(\omega, \tau)$  and  $\tilde{E}_{\text{sig}}(\omega, \tau)$  values.

Parents can pass genes onto future generations in three different ways. The three different passing methods are known as inheritance, mutation, or crossover. Inheritance involves passing genes to a child without changing the genes, mutation occurs when the parents pass genes that have been slightly modified in a random way, and crossover involves the mixing of multiple parents' genes to create the genome of the child. The portions of the next generation that are created through inheritance, mutation, and crossover can be declared by passing the desired ratios into the genetic algorithm function when it is called (Yang, 2010, p. 15031). This new generation goes through the same process described above. However, the initial electric field estimates will no longer be randomly generated. They will be generated by the current generation. Those electric field

estimates will be transformed into  $\tilde{E}_{\text{sig}}(\omega, \tau)$ , and will again be evaluated by the fitness function. The number of generations allowed can also be controlled by a parameter passed into the genetic algorithm program.

When the maximum number of generations is reached in this pulse reconstruction application, the iterative reconstruction will then take the fittest individual and finish the remainder of the iterative reconstruction algorithm. When the iterative reconstruction is completed for the most fit individual, the pulse's phase and duration information will be displayed. If one chooses an initial electric field estimate that is close to the experimental pulse's electric field, the total reconstruction process would converge more quickly. The general idea behind genetic algorithms is that as the generations progress, they will become increasingly fit as is defined by the fitness function (Yang, 2010, p. 15031).

However, this implementation of a genetic algorithm was found to be inefficient in regards to pulse reconstruction. Choosing a more accurate initial  $E(t)$  does not have a large enough impact on the reconstruction time, and there are already search algorithms available that provide results more quickly and efficiently than those from a genetic algorithm. Nevertheless, by implanting the iterative reconstruction program into a genetic algorithm in a different manner with a stronger focus on the reduction of parameters, it has been found to increase the efficiency and speed of reconstruction (Rundquist, 2002, p. 2476). Another issue with the use of a genetic algorithm in this application is that the ultrashort pulses are typically unimodal. The single peak of ultrashort laser pulses detracts from one of the main services of genetic algorithms which is to locate a global maximum or minimum.

## Results

The main goal of this research project was to cross check an aligned, student-built HITS FROG with a commercially built KM Labs FROG. By comparing the FROG's results, one can tell if the outputted pulse information is reliable and accurate. By keeping the laser, laser grating, day, and approximate location constant, it was acceptable to compare the outputs from two FROGs and expect similar results. By running the experiment described above in the procedure section and using the pulse reconstruction software that came with each FROG, the results from the two FROGs were as follows in Table 1. Fig. 15 and Fig. 16 are screenshots of the HITS FROG's output pulse reconstruction image and electric field plot respectively. Fig. 17 and Fig. 18 are screenshots of the commercial KM Labs FROG's output pulse reconstruction image and electric field plot respectively. The most important measurement to the research group was the temporal FWHM measurement, or pulse duration in time.

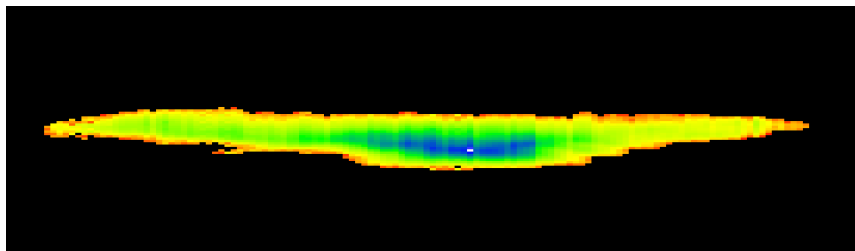


Figure 15. The above figure is the image of the ultrashort laser pulse reconstructed by the HITS FROG. Note the slight asymmetry of the pulse.

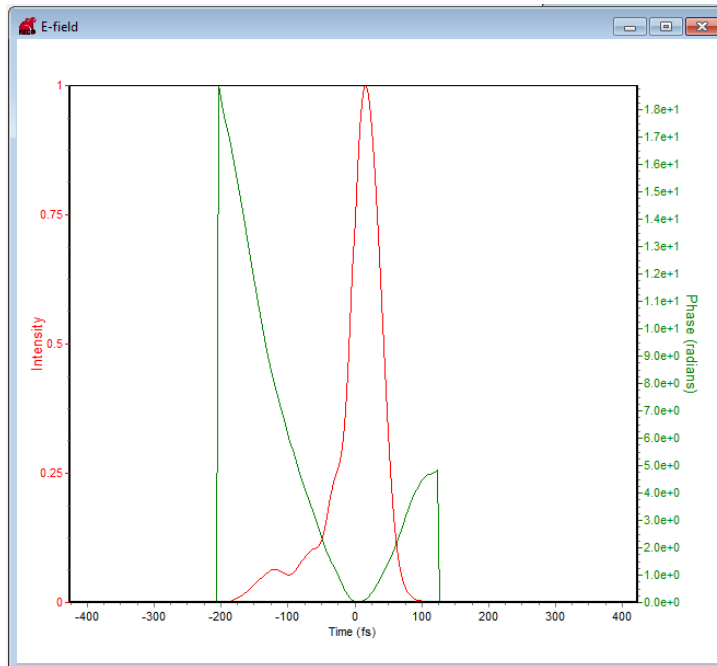


Figure 16. The above figure is a screenshot of the reconstructed electric field in time of the ultrashort laser pulse that the HITS FROG recorded. The green line is the recorded evolution of the phase throughout the overlap, and the red line shows the intensity evolution of the pulse throughout the overlap. Note that the phase appears to be quadratic, and the intensity of the pulse seems to be asymmetric.

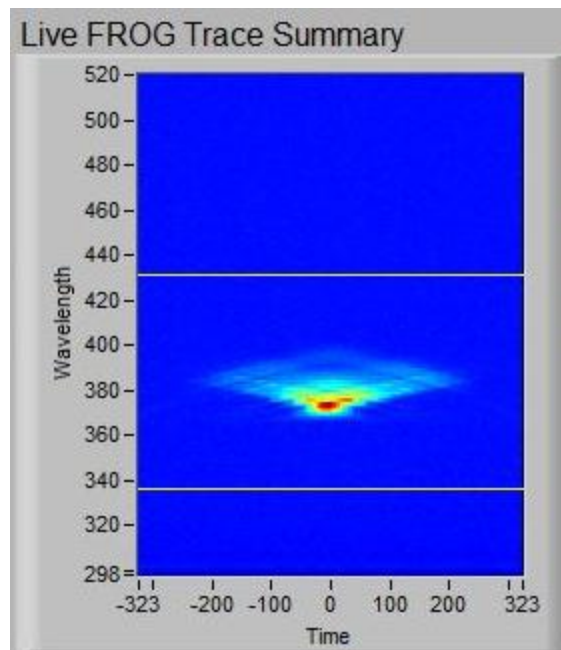


Figure 17. The above figure the image of the ultrashort laser pulse reconstructed by the KM Labs FROG.

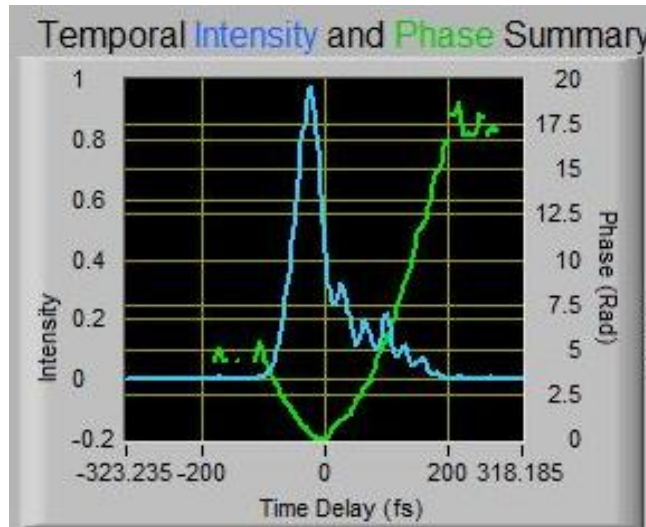


Figure 18. The above figure is a screenshot of the reconstructed electric field in time of the ultrashort laser pulse that the KM Labs FROG recorded. The green line is the recorded evolution of the phase throughout the overlap, and the blue line shows the intensity evolution of the pulse throughout the overlap. Note that the phase appears to be quadratic, and the intensity of the pulse seems to be asymmetric.

	<b>HITS</b>	<b>KM</b>	<b>Percentage Difference</b>
<b>Temporal FWHM (fs)</b>	50.9	49.4	3.0
<b>Spectral FWHM (nm)</b>	38.5	42.8	10.5
<b>FWHM TBP</b>	1.08	1.06	1.4
<b>FROG ERROR</b>	0.013	0.015	

Table 1: The table above summarizes the final measurements retrieved by the HITS FROG in comparison to those of the commercially built KM Labs FROG. The FROG error values, 1.3% and 1.5%, were produced by the separate pulse retrieval programs that came with each FROG apparatus. The percentage difference values were calculated to show the variation between the same measurements recorded by the different FROGs.

### Analysis

The temporal FWHM measurement yields the duration of the reconstructed pulse in the time domain. The HITS FROG retrieved a pulse 50.9 fs long, while the KM Labs FROG

retrieved a 49.4 fs long ultrashort pulse. The percentage difference between these two measurements is approximately 3%. The spectral FWHM measurement is the duration of the pulse in the frequency domain. The HITS FROG retrieved a pulse with a spectral width of 38.5 nm, and the KM Labs FROG retrieved a pulse with a spectral width of 42.8 nm. The percentage difference between those two measurements is higher and approximately 10.5%. The FWHM time-bandwidth product (TBP) is the product of the temporal and spectral widths of a pulse. This measurement tells the user how close the pulse is to being transform limited. The HITS FROG retrieved a FWHM TBP of 1.08, while the KM Labs FROG retrieved a FWHM TBP of 1.06 for the ultrashort laser pulse used in the experiment. The percentage difference between these measurements was approximately 1.4%.

The resulting SHG FROG errors are higher than desired. SHG FROG error values are expected to be less than 0.5% (Trebino, 1997, p. 3291). The high FROG error values from this experiment mean that the pulse retrieval programs did not reconstruct a pulse close enough to the experimentally recorded ultrashort pulse.

An asymmetric trace was noticed in the reconstructed HITS FROG pulse shown in Fig. 15. The overlapping split pulses are expected to be symmetric because the pulses are identical aside from the time delay. This semi-identical nature of the overlapped pulses theoretically requires a symmetric SHG pulse. It was hypothesized that this asymmetry was due to some sort of limiting factor only affecting one of the initial laser pulses. This could be an issue with one of the mirrors of the FROG apparatus. A chirped pulse can be ruled out as the cause of this aberration because the phase was already retrieved, is known to exist in the pulse, and is ambiguous in SHG pulse reconstructions.

## **FROG Error**

Generally, FROGs are extremely accurate due to the very few approximations that are required in order to read and interpret the pulse. One assumption that is commonly made with FROGs is that they use nearly instantaneous response media. However, that assumption and any other systematic errors in measurement can be modeled in the algorithm that retrieves the pulse. Situations requiring algorithm modification typically only occur when the pulses are less than 10 femtoseconds or significantly complex (Trebino, 2000, p. 110). In both the HITS and KM Labs FROGs, the response of the medium was faster than the pulses recorded, and there were not parts of the phase-retrieval algorithm that needed to be modified.

## **Future Work**

A goal for the HITS FROG at Kansas State University is to decrease the 1.5 fs difference between the retrieved pulse duration values from the HITS FROG and the KM Labs FROG. Since the algorithms used by each of the FROG programs were unobtainable, it is impossible to know if there were any differences within the reconstruction algorithms that could have caused the pulse duration discrepancy. Using a single reconstruction program to evaluate both traces could eliminate this possible source of reconstruction measurement discrepancy.

There are still other aspects of the HITS FROG that could be modified in order to decrease the difference in retrieved pulse durations. Due to time constraints, the issue of recording an asymmetric pulse was not further explored. Adjusting the delay stage mirrors has major effects on the delayed beam's location, and therefore it was typically avoided

during the initial alignment process. However, by making small modifications to the delay stage's mirrors, a more symmetric pulse trace could possibly be obtained. Fixing the above issues could potentially lead to more consistent results produced by the HITS FROG.

## Appendix: Significance of Variables Used in the Iterative Reconstruction Algorithm

Variable	Significance
$E(t)$	Electric field amplitude in time of the stationary 800 nm pulse
$E(t - \tau)$	Electric field amplitude in time of the delayed 800 nm pulse
$E_{\text{sig}}(t, \tau)$	Electric field amplitude in time of the 400 nm signal pulse
$\Sigma_g^E(\omega, \tau)$	Spectrogram of the 400 nm signal pulse experimentally collected during a FROG trace
$I_{\text{FROG}}(\omega, \tau)$	Experimentally collected intensity data from the 400 nm signal pulse of a FROG trace in the frequency domain
$\tilde{E}_{\text{sig}}(\omega, \tau)$	Fourier-transformed electric field amplitude in frequency of the 400 nm signal pulse
$\tilde{E}'_{\text{sig}}(\omega, \tau)$	Improved Fourier-transformed electric field amplitude in frequency of the 400 nm signal pulse
$E'_{\text{sig}}(t, \tau)$	Improved electric field amplitude in time of the 400 nm signal pulse
$E^{(k+1)}(t)$	Electric field amplitude estimate in time for the $k+1$ iteration of the reconstruction algorithm
$G^{(k)}$	FROG error or root-mean-square difference between the experimentally measured trace and the computed trace at iteration $k$ of the reconstruction algorithm
$I_{\text{FROG}}(\omega_i, \tau_j)$	Experimentally collected intensity value at frequency pixel $i$ , and time pixel $j$
$I_{\text{sig}}^{(k)}(\omega_i, \tau_j)$	Computed intensity value at frequency pixel $i$ , and time pixel $j$ in the reconstructed pulse at the $k$ -th iteration of the reconstruction algorithm

## References

- DeLong, K. W., Trebino, R., Hunter, J., & White, W. E. (1994). Frequency-resolved optical gating with the use of second-harmonic generation. *Journal of the Optical Society of America B*, 11(11), 2206-2215.
- Diels, J.-C., & Rudolph, W. (1996). *Ultrashort Laser Pulse Phenomena Fundamentals, Techniques, and Applications on a Femtosecond Time Scale* (Chapter 6).
- Rundquist, A., & Efimov, A. (2002). Pulse shaping with the Gerchberg-Saxton algorithm. *Journal of the Optical Society of America B*, 19(10), 2468-2478.
- Sullivan, A., White, W. E., Chu, K. C., Heritage, J. P., DeLong, K. W., & Trebino, R. (1996). Quantitative investigation of optical phase-measuring techniques for ultrashort pulse lasers. *Journal of the Optical Society of America B*, 13(9), 1965-1978.
- Sumner, Thomas. (2012). Beam's brief duration could help scientists glimpse the atomic world. *Inside Science News Service*. Retrieved from <http://www.insidescience.org/content/shortest-laser-pulse-ever-created/794>
- Trebino, R. (2000). *Frequency-Resolved Optical Gating: The Measurement of Ultrashort Laser Pulses*. Boston: Kluwer Academic Publishers.
- Trebino, R. (2014a). *Ultrafast Optics Course – The Generation of Ultrashort Laser Pulses*. Retrieved from <http://frog.gatech.edu/talks.html>
- Trebino, R. (2014b). *Ultrafast Optics Course – Ultrashort Laser Pulses I*. Retrieved from <http://frog.gatech.edu/talks.html>
- Trebino, R. (2014c). *Ultrafast Optics Course – Nonlinear Optics*. Retrieved from <http://frog.gatech.edu/talks.html>

- Trebino, R. (2014d). *Ultrafast Optics Course – Measuring Ultrashort Laser Pulses I - Autocorrelation*. Retrieved from <http://frog.gatech.edu/talks.html>
- Trebino, R. (2014e). *Ultrafast Optics Course – Measuring Ultrashort Laser Pulses II - FROG*. Retrieved from <http://frog.gatech.edu/talks.html>
- Trebino, R., DeLong, K. W., Fittinghoff, D. N., Sweetser, J. N., Krumbugel, M. A., Richman, B. A., & Kane, D. J. (1997). Measuring ultrashort laser pulses in the time-frequency domain using frequency-resolved optical gating. *Review of Scientific Instruments*, 68(9), 3277-3295.
- Wong, T. C., & Trebino, R. Single-frame measurement of complex laser pulses tens of picoseconds long using pulse-front tilt in cross-correlation frequency-resolved optical gating. *Journal of the Optical Society of America B*, 30(11), 2781-2786.
- Yang, W., Springer, M., Strohaber, J., Kolomenski, A., Schuessler, H., Kattawar, G., & Sokolov, A. (2010). Spectral phase retrieval from interferometric autocorrelation by a combination of graduated optimization and genetic algorithms. *Optics Express* 18(14), 15028-15038.